DALTON

Cascade complexation of pseudo-halide by dicopper cryptates: a linear Cu–NNN–Cu unit†

Charles J. Harding,[a] Frank E. Mabbs,[b] Eric J. L. MacInnes,[b] Vickie McKee *[,c] and Jane Nelson *[,a,c]

[a] *Chemistry Department, Open University, Milton Keynes MK7 6AA, UK*
[b] *EPSRC c.w. EPR Service Centre, Chemistry Department, The University of Manchester, Oxford Road, Manchester M13 9PL, UK*
[c] *School of Chemistry, Queen's University of Belfast, Belfast BT9 5AG, UK*

An X-ray crystallographic structure determination of a μ-azido azacryptate has confirmed the existence of collinear Cu–NNN–Cu geometry, earlier cited as the origin of unusual spectroscopy in dicopper μ-azido cryptates; the isoelectronic μ-cyanato cryptate is also isostructural.

Increasing interest[1] in anion co-ordination chemistry has emphasised the value of two main receptor types. Protonated amine or guanidinium receptors present a dual recognition system consisting of a convergently directed electrostatic field together with specific hydrogen-bond interactions. In the second type, dinuclear cationic complexes also provide an electrostatic field, deriving from the pair of positively charged cations, while the hydrogen-bond interactions are replaced by geometrically well defined co-ordinate bonds to each donor site from the bridging anion. This ('cascade') receptor[1b,1c] is likely to be most effective for potentially bridging bidentate anions, while large polyoxo or halogeno anions may prefer protonated amine salts offering more than two hydrogen-bond donor recognition sites.

Pseudo-halide anions are good candidates for the 'cascade' type of complexation between cations in dinuclear complexes; they have the further advantage of being spectroscopically informative *via* electronic[2] and/or vibrational[3] spectra about their co-ordination mode. In the case of thiocyanate, for example, infrared spectra alone can, to a first approximation, distinguish terminal co-ordination through N or S from N,S or N-only bridging. Although electronic charge-transfer spectra can be informative about the co-ordination mode of azide, vibrational spectra are normally insensitive to it and no generally accepted criteria exist to distinguish the various possible bridging/terminal modes for either azide or cyanate anions. Where dinuclear macrocyclic or acyclic complexes act as hosts for azide ions the latter have the option of adopting 1,1- or 1,3-bridging modes (**I** and **II**). The CuNCu or CuNNNCu skeletons revealed by X-ray crystallography are invariably bent[1c,4] with the Cu–N–N angle approximately trigonal. However, the ellipsoidal cavity provided by cryptate hosts is not conducive to the adoption of a non-linear geometry for a bridging ligand.

Following the development of a facile synthetic route[5,6] to azacryptands, we have investigated the co-ordination chemistry of a range of hexa(Schiff base) cryptands[2,7–10] **IV** and their BH_4^--reduced octaamino derivatives **V** as hosts for copper-(I) and -(II). While the softer sp^2 N-donor iminocryptands favour the copper(I) oxidation state,[11] we have been able to generate many dicopper(II) cryptates of the aminocryptands,[2,7–10] often incorporating bridging anions OH^-, imidazolate or azide in cascade fashion between the cations.

We have shown that aminocryptands when protonated represent useful receptors for oxo- or perfluoro-anions,[12] on account of the many possible hydrogen-bond interactions between the host and guest. A similarly inclusive anion cryptate has been structurally characterised for the protonated bis[tris(2-aminoethyl)amine] azide complex.[13] The dinuclear metal(II) cryptates of many of the aminocryptand series also make good hosts for cascade complexation of anionic, particularly pseudo-halide, guests, although full structural characterisation[2] of a μ-azido cryptate has until now proved elusive. The dinuclear monoazido cryptates which have been obtained show characteristic and unusual spectroscopic signatures which we have attributed to enforced collinearity of the M–NNN–M assembly[2,7–9] (bridging mode **III**). One particularly striking feature is the appearance of $\nu_{asym}(N_3^-)$ at wavenumbers well outside the normal range, approximately 100 cm^{-1} higher than those observed for bridged or terminal azido complexes.

In the present work we have synthesised an isoelectronic cyanato complex, which again shows the pseudo-asymmetric stretching mode of pseudo-halide $\nu_{asym}(NCO^-)$ at 2306 cm^{-1}, well above the normally accepted range (2150–2250 cm^{-1}).[14] One possible common explanation of shifts to higher energy for pseudo-halide NXY stretching frequencies is the existence of

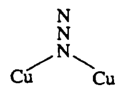

I

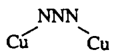

II

Cu—NNN—Cu

III

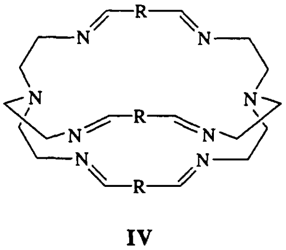

IV

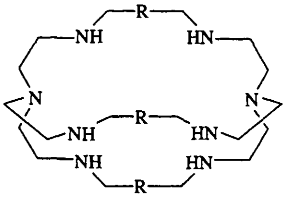

V

---

† *Supplementary data available* (No. SUP 57151, 4 pp.): observed and calculated magnetic susceptibilities. See Instructions for Authors, *J. Chem. Soc., Dalton Trans.*, 1996, Issue 1.

Non-SI unit employed: $\mu_B \approx 9.27 \times 10^{-24}$ J T^{-1}.

large adjacent bond interactions of mechanical rather than electronic origin,[15] arising from collinear disposition of vectors in the M–NXY–M assembly.

Results and Discussion

We are now able to confirm *via* X-ray crystallographic structure determination of $[Cu_2(N_3)L^1][ClO_4]_3\cdot MeCN\cdot 1.5EtOH$ **1a** and $[Cu_2(NCO)L^1][ClO_4]_3\cdot MeCN\cdot 1.5EtOH$ **2** the hypothesis of collinear M–NXY–M geometry. Fig. 1 shows the structure of the cations, which are isostructural. The copper ions in **2** are each co-ordinated to four amine nitrogen atoms and to the bridging cyanate ion. The geometry at Cu(2) approximates to a trigonal bipyramid but Cu(1) has a less regular environment ['trigonal' angles 126, 122, 109 and 108, 107, 140° at Cu(2) and Cu(1) respectively]. This difference may be due to the orientation of the secondary amine groups relative to the unique aromatic CH *ortho* to both CH_2NH substituents, which is *trans* in all cases except for N(32).

The cyanate ion appears disordered between the Cu(1)–NCO–Cu(2) and Cu(1)–OCN–Cu(2) orientations. It was refined with a 50% contribution from each arrangement and this model is supported by the very similar atomic displacement parameters for the O/N atoms (Fig. 1). The cyanate is approximately linear but the Cu–O/N–C bonds are slightly bent.

The potential three-fold symmetry of the cation is broken by the differential geometry in the strand carrying N(32) and N(31) and by the almost parallel orientation of two of the phenyl rings [C(16)–C(21) and C(28)–C(33), interplanar angle 15.5°]. This permits a π–π interaction between the C(28)–C(33) rings of neighbouring ions (interplanar distance 3.4 Å), a less well aligned interaction between pairs of C(4)–C(9) rings (3.5 Å) and two edge-to-face interactions [C(8) to the centroid of the neighbouring C(16)–C(21) ring, 3.75 Å]. These interactions can be seen in the packing diagram (Fig. 2). None of the phenyl rings can be reasonably described as lying over the encapsulated cyanate but there is a suggestion of an intramolecular π–π interaction (2.9–3.5 Å from the phenyl planes to the cyanate).

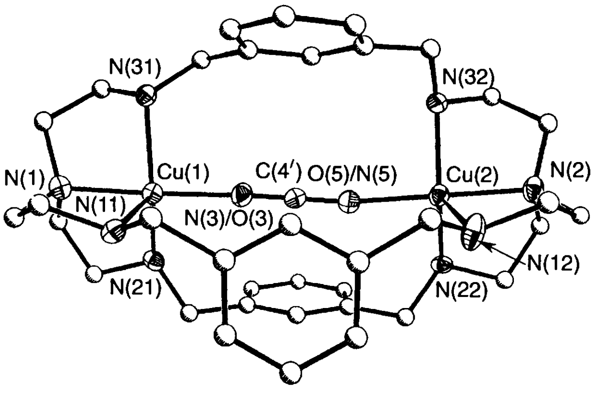

Fig. 1 Structure of the cation in complex **2**, showing 30% thermal ellipsoids for non-carbon atoms (**1a** is isomorphous). Selected bond lengths (Å) and angles (°): Cu(1)–O(3)/N(3) 1.925(5), Cu(2)–N(5)/O(5) 1.947(5); Cu(1)–O(3)/N(3)–C(4′) 168.8(5), Cu(2)–N(5)/O(5)–C(4′) 172.2(4), O(3)/N(3)–C(4′)–N(5)/O(5) 178.5(6)

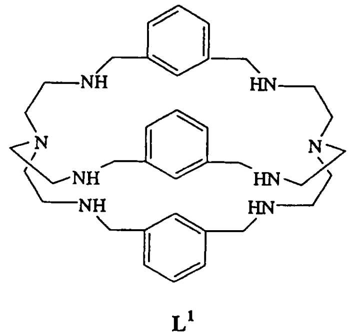

L^1

The asymmetric unit also contains three perchlorate anions, one acetonitrile solvate molecule and 1.5 molecules of ethanol. One of the perchlorate ions is severely disordered, and the full-occupancy ethanol molecule is disordered between two orientations. The only notable interaction between the cation and either anions or solvate molecules is the 2.70(1) Å hydrogen bond between N(12) and O(31′) (under symmetry transformation $-x, y - \frac{1}{2}, \frac{1}{2} - z$).

The azido cryptate **1** is isomorphous with the cyanate and has been refined using the same coordinates. Poor crystal quality resulted in higher estimated standard deviations for the geometric parameters of the azide structure; however, no significant differences were observed.

We have previously noted complex X-band EPR spectra which characterise the putatively linear μ-azido-dicopper cryptates,[2,7–9] the most noticeable feature of which is an intense low-field signal. The corresponding spectrum of **1a** shows these effects (Fig. 3), although to a less marked extent than do some of the other cryptates. The Q-band spectrum of **1a** (Fig. 4) displays a much simpler pattern than that at X-band, but still contains features which are compatible with an $S = 1$ state with zero-field splitting. The cyanato-bridged cryptate **2** does not show the intense low-field feature observed for the analogous collinear azido-bridged system; instead (Fig. 3) its X-band EPR spectrum appears as a featureless *g ca.* 2 signal, with a very weak feature at half-field with *ca.* 10^{-2} times the intensity of the main signal. At Q-band (Fig. 4) some splitting of the $g = 2$ signal is seen together with a very weak feature at half-field. These X- and Q-band spectra are compatible with a small ($\ll h\nu$ at X-band) zero-field splitting.

Qualitatively the X- and Q-band spectra on both complexes **1a** and **2** are consistent with a significantly larger zero-field splitting in **1a** compared to **2**. Further multifrequency EPR experiments and spectral simulations are in progress[16] to establish the spin-Hamiltonian parameters for these systems. The differences in the zero-field splittings arise from different efficiencies of the excited-state pathway between the copper(II) paramagnets provided by the different bridging groups.

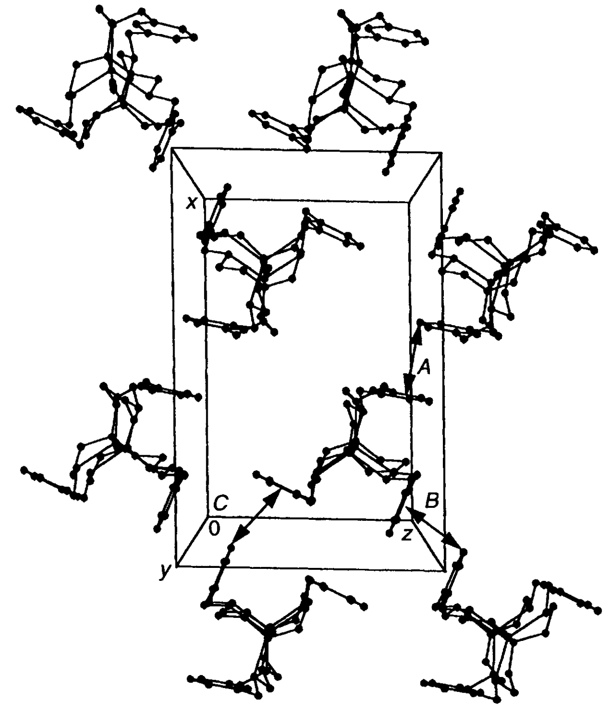

Fig. 2 Packing diagram for complex **2** with anions and solvate omitted for clarity. Dimensions: $A = 3.4$, $B = 3.5$, $C = 3.75$ Å

Variable-temperature magnetic susceptibility studies indicate only slight interaction which appears to be in opposite senses for the two complexes, *i.e.* ferromagnetic for **1** and antiferromagnetic for **2**. The data were fitted by the Bleaney–Bowers equation (1), modified by the inclusion of a Weiss

$$\chi_m = [Ng^2\beta^2/3k(T-\theta)][1+\tfrac{1}{3}\exp(-2J/kT)]^{-1}(1-p) + (pNg^2\beta^2/4kT) + N\alpha \qquad (1)$$

temperature θ to allow for intermolecular exchange and a term p which is the fraction of any paramagnetic impurity. The best fits gave the values $g = 2.13$, $-2J = 7$ cm^{-1}, $p = 0.04$ for **2** (Fig. 5), and $g = 2.13$, $-2J = -15$ cm^{-1}, $\theta = 1.5$ K for **1a** (Fig. 6) (see SUP 57151). In each case, the temperature-independent paramagnetism $N\alpha$ was set at 60×10^{-6} cm^3 mol^{-1} per Cu. Likewise weak ferromagnetic exchange is also evident in **1b**, the corresponding $CF_3SO_3^-$ salt of **1a**, previously described,[7] for which $g = 2.13$, $-2J = -10$ cm^{-1} (Fig. 7). An interesting difference in the magnetic behaviour of these two salts of the azide complex is apparent from Figs. 6 and 7. Whereas the $CF_3SO_3^-$ salt shows no evidence of interdimer interaction ($\theta = 0$), the decrease in magnetic moment below 10 K for the ClO_4^- salt requires an (antiferromagnetic) interdimer exchange term in equation (1). Presumably this interaction operates *via* the stacking arrangement of adjacent cryptate ions (Fig. 2). The integrated EPR signal intensity for **1a** and **2** rises regularly with decreasing temperature to 4 K, with the increase being greater for the azido- than for the cyanato-bridged complex, compatible with the magnetic susceptibility data.

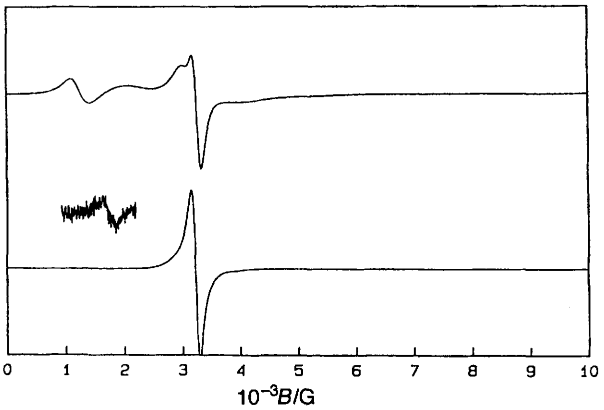

Fig. 3 First-derivative EPR spectra at 100 K and X-band frequency of complexes **1a** (top) and **2** (bottom). Microwave frequency 9.636 GHz; modulation frequency and amplitude, 100 kHz and 1 mT; microwave power, 10 mW. Inset: gain × 64

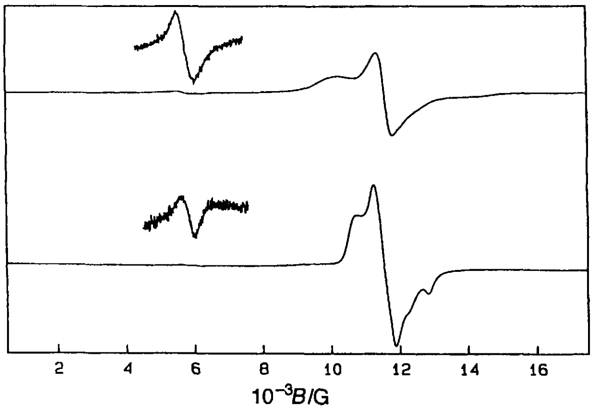

Fig. 4 First-derivative EPR spectra at 4 K and Q-band frequency of complexes **1a** (top) and **2** (bottom). Microwave frequency, 34.20 GHz; modulation frequency and amplitude, 100 kHz and 1 mT; microwave power, 0.5 mW. Insets: top, gain × 8; bottom, gain × 32

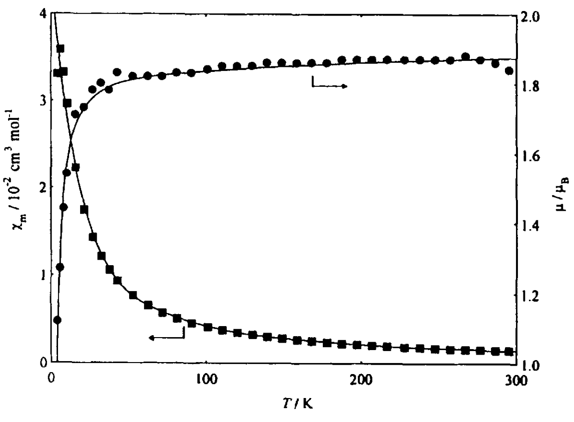

Fig. 5 Temperature variation of the molar magnetic susceptibility and effective magnetic moment per Cu of $[Cu_2(NCO)L^1][ClO_4]_3 \cdot 2H_2O$ **2**. The solid lines are the best fit using equation (1) (see text for parameters)

The most probable interpretation of the EPR spectral and magnetic susceptibility data for complex **1** is a small stabilisation of the triplet relative to the singlet state, leading to an $S = 1$ ground state. Despite the isoelectronic nature of the ligands, and isostructural nature of the complexes, a triplet ground state does not seem to be the consequence of collinear geometry in the μ-cyanato-dicopper(II) assembly in **2**.

Conclusion

The hitherto unknown collinear M–NNN–M geometry, previously suggested for a number of μ-azido cryptates on the basis of unusual spectroscopic properties, has been confirmed for one member of the series by an X-ray crystallographic

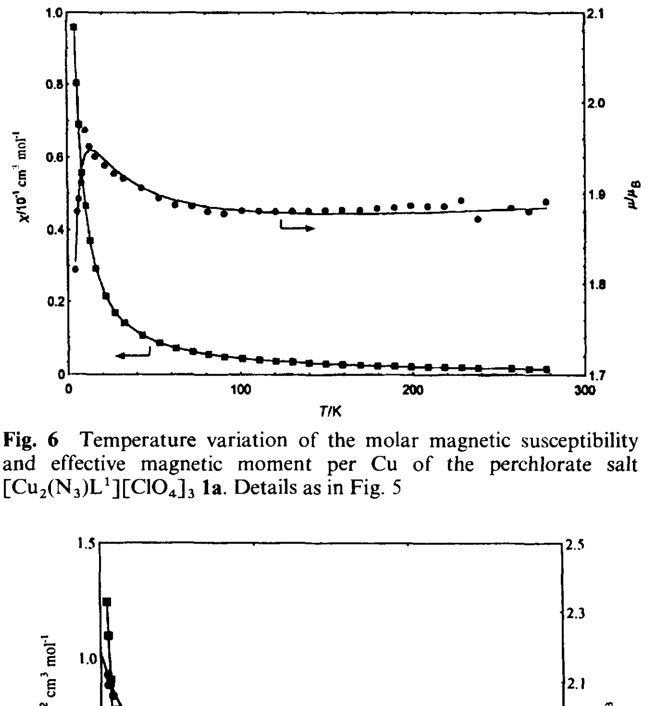

Fig. 6 Temperature variation of the molar magnetic susceptibility and effective magnetic moment per Cu of the perchlorate salt $[Cu_2(N_3)L^1][ClO_4]_3$ **1a**. Details as in Fig. 5

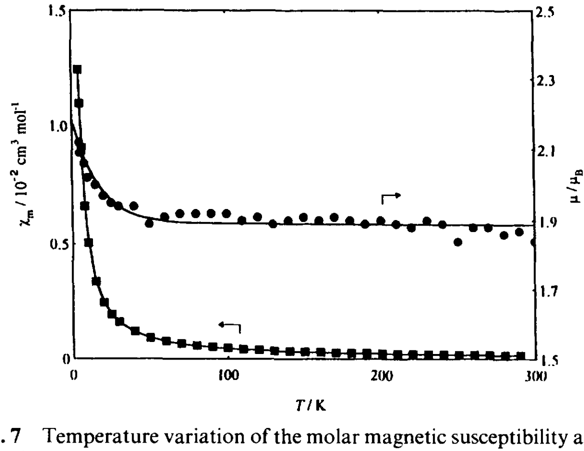

Fig. 7 Temperature variation of the molar magnetic susceptibility and effective magnetic moment per Cu of the triflate salt $[Cu_2(N_3)L^1][CF_3SO_3]_3$ **1b**. Details as in Fig. 5

structure determination. The isostructural μ-cyanato cryptate shows a similar increase in the asymmetric $v_{asym}(NXY)$ pseudo-halide stretching frequency, but does not show the unusual EPR spectrum and weak ferromagnetic exchange interaction characteristic of collinear μ-azido cryptates.

Experimental

Preparation of $[Cu_2(NXY)L^1][ClO_4]_3 \cdot xH_2O$ (X = Y = N, x = 0 1a; X = C, Y = O, x = 2 2)

To L^1 (0.1 mmol), prepared as described,[8] dissolved in EtOH (10 cm^3) was added $Cu(ClO_4)_2 \cdot 6H_2O$ (0.2 mmol) in MeCN (5 cm^3) and sodium pseudo-halide salt (0.1 mmol) dissolved in a few drops of water. On standing, a green (**1a**) or blue-green (**2**) microcrystalline product was obtained in ≈60% yield. For X-ray crystallography the product was recrystallised from MeCN–EtOH in an atmosphere of MeOH [Found (Calc.): **1a**, C, 40.5 (40.5); H, 5.1 (5.0); N, 13.9 (14.4). **2**, C, 40.4 (40.5); H, 5.1 (5.2); N, 11.4 (11.5)%]. Magnetic moments: **1a**, 1.89 (300); 1.97 (10); **1b**, 1.84 (300); 2.02 (10); **2**, 1.91 (300); 1.53 μ_B (10 K).

X-ray crystallography

Crystal data for complex 2. $C_{42}H_{66}Cl_3Cu_2N_{10}O_{14.5}$ blue-green block, dimensions 0.90 × 0.57 × 0.50 mm, monoclinic, space group $P2_1/c$, $a = 16.905(2)$, $b = 27.945(3)$, $c = 10.876(2)$ Å, $\beta = 91.27(1)°$, $U = 5137(1)$ Å^3, $\mu = 1.06$ mm^{-1}, $Z = 4$, $F(000) = 2452$.

Data were collected at 153 K on a Siemens diffractometer using graphite-monochromated Mo-Kα radiation ($\lambda = 0.710\,73$ Å). 9755 Reflections were collected in the range $4 < 2\theta < 45°$, 9012 unique reflections ($R_{int} = 0.0168$) being used in the refinement. An empirical absorption correction based on ψ-scan data was applied ($T_{max} = 0.797$, $T_{min} = 0.735$). The structure was refined using coordinates from the isomorphous azide. Hydrogen atoms were inserted at calculated positions with isotropic thermal parameters except those of the disordered solvate molecules which were not included. All the data were used for refinement of 685 parameters on F^2 which converged with $wR2 = 0.1932$, goodness of fit = 1.048 [conventional $R = 0.0638$ for $I > 2\sigma(I)$] $\{w = 1/[\sigma^2(F_o^2) + (0.0919P)^2 + 16.45P]$, where $P = [\max(F_o^2, 0) + 2F_c^2]/3\}$.

Crystal data for complex 1a. $C_{41}H_{66}Cl_3Cu_2N_{12}O_{13.5}$, green plate, dimensions 0.40 × 0.32 × 0.12 mm, monoclinic, space group $P2_1/c$, $a = 16.53(2)$, $b = 27.33(4)$, $c = 10.68(1)$ Å, $\beta = 90.90(3)°$, $U = 4826(10)$ Å^3, $\mu = 1.126$ mm^{-1}, $F(000) = 2452$. 4811 Reflections ($R_{int} = 0.068$) were used in the refinement. The structure was solved by Patterson methods[17] and refined as described above. An empirical absorption correction based on ψ-scan data was applied ($T_{max} = 0.978$, $T_{min} = 0.709$). The poor quality of the data set [2132 reflections > $2\sigma(I)$] meant that the refinement converged at $wR2 = 0.2572$, goodness of fit 1.096 [conventional $R = 0.91$ for $I > 2\sigma(I)$] $\{w = 1/[\sigma^2(F_o^2) + (0.10000P)^2 + 22.00P]$, where $P = [\max(F_o^2, 0) + 2F_c^2]/3\}$. All programs used in the structure refinement are contained in the SHELXL 93[18] package.

Atomic coordinates, thermal parameters, and bond lengths and angles have been deposited at the Cambridge Crystallographic Data Centre (CCDC). See Instructions for Authors, *J. Chem. Soc., Dalton Trans.*, 1996, Issue 1. Any request to the CCDC for this material should quote the full literature citation and the reference number 186/125.

Magnetic susceptibility measurements

Magnetic susceptibility data were recorded using an Oxford Instruments Faraday balance equipped with a liquid-helium cryostat. The sample size was typically 30 mg and the field strength 0.8 T. At each temperature, an average of 36 data points was recorded. The balance was calibrated using $Hg[Co(NCS)_4]$. Corrections were made for the diamagnetism of the Teflon sample holder and the diamagnetic contribution of the sample using Pascal's constants.

EPR spectroscopy

The EPR spectra of powdered samples of complexes **1** and **2** were obtained using a Bruker ESP 300E spectrometer, in the temperature range 300–100 K at X-band and 100–2 K at Q-band frequencies. The cooling at X-band was *via* the Bruker BVT 2000 variable-temperature unit and at Q-band *via* an ER 5106QT low-temperature resonator and an Oxford Instruments CF 935 cryostat. The variation of the spectral intensities with temperature at Q-band, in the range 2–100 K, was determined by double integration using the Bruker integration software. The spectra were obtained using non-saturating microwave powers. For **1a** the spectra were integrated over the magnetic field range 50–1650 mT, but because of problems with the baseline over this extended field range that for **2** was restricted to 750–1550 mT.

References

1 (*a*) B. Dietrich, *Pure Appl. Chem.*, 1993, **65**, 1457; (*b*) P. G. Potvin and J.-M. Lehn, *Prog. Macrocyclic Chem.*, 1987, 167; (*c*) J.-M. Lehn, *J. Am. Chem. Soc.*, 1982, **104**, 167.

2 M. G. B. Drew, J. Hunter, C. J. Harding, D. J. Marrs and J. Nelson, *J. Chem. Soc., Dalton Trans.*, 1992, 3235.

3 C. J. Harding, D. McDowell, J. Nelson, S. Raghunathan, C. Stevenson, M. G. B. Drew and P. C. Yates, *J. Chem. Soc., Dalton Trans.*, 1990, 7453.

4 V. McKee, C. A. Reed, J. V. Dagdigian and R. Bau, *J. Am. Chem. Soc.*, 1983, **103**, 7000; Y. Agnus, R. Weiss and R. Louis, *J. Am. Chem. Soc.*, 1983, **101**, 3381.

5 J. Jazwinski, J.-M. Lehn, D. Lilienbaum, R. Zeissel, J. Guilheim and C. Pascard, *J. Chem. Soc., Chem. Commun.*, 1987, 1691.

6 D. McDowell and J. Nelson, *Tetrahedron Lett.*, 1988, 385.

7 Q. Lu, J.-M. Latour, C. J. Harding, N. Martin, D. Marrs, V. McKee and J. Nelson, *J. Chem. Soc., Dalton Trans.*, 1994, 1471.

8 C. J. Harding, Q. Lu, D. J. Marrs, N. Martin, V. McKee and J. Nelson, *J. Chem. Soc., Dalton Trans.*, 1995, 1739.

9 O. W. Howarth, C. J. Harding, Q. Lu, D. J. Marrs, G. G. Morgan, V. McKee and J. Nelson, *J. Chem. Soc., Dalton Trans.*, 1996, 3021.

10 D. Marrs, Q. Lu, V. McKee and J. Nelson, *Inorg. Chim. Acta*, 1993, **211**, 195.

11 Q. Lu, M. McCann and J. Nelson, *J. Inorg. Biochem.*, 1993, 633.

12 G. G. Morgan, V. McKee and J. Nelson, *J. Chem. Soc., Chem. Commun.*, 1995, 1649.

13 B. Dietrich, J. Guilheim, J.-M. Lehn, C. Pascard and E. Sonveaux, *Helv. Chim. Acta*, 1984, **67**, 91.

14 K. Nakamoto, *Infrared and Raman Spectra of Inorganic and Coordination Compounds*, 3rd edn., Wiley, New York, 1978, p. 276.

15 M. G. B. Drew, B. P. Murphy, J. Nelson and S. M. Nelson, *J. Chem. Soc., Dalton Trans.*, 1987, 873.

16 C. J. Harding, F. E. Mabbs, E. J. L. MacInnes and J. Nelson, unpublished work.

17 G. M. Sheldrick, SHELXS 86, *Acta Crystallogr., Sect. A*, 1990, **46**, 467.

18 G. M. Sheldrick, SHELXL 93, University of Göttingen, 1993.

Received 18th April 1996; Paper 6/02729F